Springer

KSME

Journal of Mechanical Science and Technology 29 (1) (2015) 59~66
www.springerlink.com/content/1738-494x
DOI 10.1007/s12206-014-1209-9

Transmission loss of orthogonally stiffened laminated composite plates †

Cheng Shen, Fengxian Xin* and Tianjian Lu

State Key Laboratory for Mechanical Structure Strength and Vibration, School of Aerospace, Xi'an Jiaotong University, Xi'an 710049, China

(Manuscript Received April 8, 2014; Revised July 8, 2014; Accepted July 16, 2014)

Abstract

Sound transmission through laminated composite plates reinforced by two sets of orthogonal stiffeners is investigated theoretically. A layerwise shear deformable theory is used to model the vibration of the laminated composite face-panel; A governing equation of I section composite beam is introduced, which accounts for the extensional, flexural, torsional and their coupling effects. The Euler-Bernoulli beam theory and torsional wave equation are employed to describe the flexural and rotational motions of the rib stiffeners, respectively. The technique of Fourier transform is applied to solve the governing equations resulting in infinite sets of simultaneous algebraic coupled equations, which are numerically solved by truncating them into a finite range insofar as the solutions converge. The accuracy of the numerical solutions is checked by comparing the present model predictions with existing literature. The validated model is subsequently employed to quantify the effects of the spacing of the stiffeners and the stacking geometry of the laminated composite face-panel and stiffeners on sound transmission through the structure. It is demonstrated that both the stiffener spacing and the stacking geometry have significant influences on the sound transmission loss across the structure. The proposed theoretical model successfully characterizes the process of sound penetration through stiffened laminated composite plates, which should be much helpful for the practical design of such structures with acoustic requirements.

Keywords: Composite plate; Layerwise theory; Orthogonal stiffeners; Transmission loss

1. Introduction

Vibroacoustic property of beam stiffened plate has been a long-standing research topic [1-9] because of its widely applications and the complexity of the problem itself. Many useful theoretical models have been built to solve the problem of stiffened plate under various operating conditions, and there are a few favorable review papers [10-12] to refer to. A few of important literatures limited to deterministic method are emphasized below to describe the state of art of investigation of orthogonally stiffened composite plate.

At the early stage, Mead and Mace have done a lot of work [2-5, 10] for stiffened plates. Among them, Mead and Pujara [2] developed a space-harmonic method to study double-leaf plates with periodic links [13]. Mace employed Fourier transform to solve the vibration response of parallel stiffened [4, 5] and orthogonally stiffened plate [3], in which only fluid loading on one side has been taken into account. As a matter of fact, both space-harmonic method and Fourier transform technique transform the governing equations into infinite sets of simultaneous algebraic equations, and then numerically solve them by truncating them into a finite range.

If composite plate was considered, the Kirchhoff assumption for thin isotropic plate is not appropriate obviously. In fact, stiffened composite plate has been widely used in applications due to the great advantage of composite material [14]. However, less attention has been paid to the sound radiation and transmission of stiffened laminated composite plates. Based on the classical laminated composite plate theory (CLPT), Yin et al. [15, 16] extended Mace's model [5] to study the parallel stiffened composite plate. Recently, a first order shear deformation theory (FSDT) is employed by Mejdi et al. [17] to consider the transverse shear strain of the base plate, where the in plane motion of the stiffeners is also accounted for. Whereas, the governing equations for stiffeners only pertain to thin-walled isotropic beam (or uncoupled composite case) while not the general composite beam.

To develop a more accurate theoretical model, the layerwise shear deformable theory is applied to model the vibration of the laminate composite base plate, and the shear deformable beam theory is utilized to model the vibration of arbitrary thin-walled composite beam stiffeners. Note that the single-layer theories (e.g. CLPT or FSDT) used by previous researchers remain acceptable for thin bare plate, which probably induce significant deviations for thicker and stiffened plates. On the basis of the present theoretical model, numeri-

*Corresponding author. Tel.: +86 29 82663223, Fax.: +86 29 82663223
E-mail address: fengxian.xin@gmail.com
† This paper was presented at the FEOFS 2013, Jeju, Korea, June 9-13, 2013.
Recommended by Guest Editor Jung-Il Song

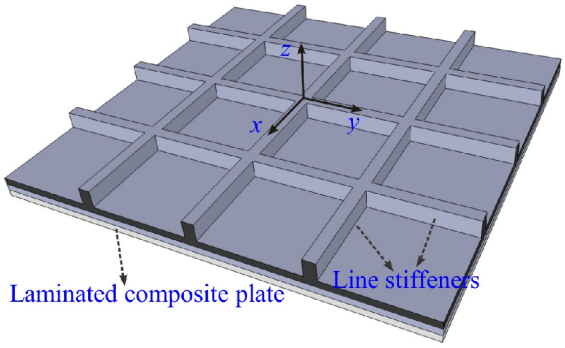

Fig. 1. Laminated composite plate reinforced by orthogonal stiffeners.

cal investigations are conducted specially focusing on the influence of stiffeners spacing and stacking geometry on the vibroacoustic property of the structure.

2. Mathematical formulation of the problem

As illustrated in Fig. 1, we consider a laminated composite plate reinforced by orthogonal stiffeners, where the two sets of stiffeners are assumed to be uniform and straight along the lines $x = ml_x$ and $y = nl_y$ (here m and n being integers) with l_x and l_y denoting stiffeners spacing, respectively. The origin of the system's coordinate is selected to be located at the junction of two sets of orthogonal stiffeners, with x-axis and y-axis aligning with line stiffeners so as to simplify the following algebra operations. The whole structure is a two dimensionally periodic structure and assumed to be immersed in acoustic fluid (e.g. air).

Following the layerwise shear deformable theory [18], the displacements of the i th layer of the composite base plate are expressed as:

$$\begin{cases} u^i(x,y,z,t) = u_0^i(x,y,t) + z\phi_x^i(x,y,t) \\ v^i(x,y,z,t) = v_0^i(x,y,t) + z\phi_y^i(x,y,t) \\ w^i(x,y,z,t) = w_0^i(x,y,t) \end{cases} \tag{1}$$

where (u_0^i, v_0^i, w_0^i) and (ϕ_x^i, ϕ_y^i) are displacement and rotation unknowns of transverse normal respectively. Notice that the present layerwise shear deformable theory model can be degraded to the FSDT model if the number of the total layers is set to be one. Under above assumptions, the governing equation of ith material layer for a fluid-loaded laminated composite structure can be expressed in the following form:

$$\begin{aligned} &\frac{\partial N_{xx}^i}{\partial x} + \frac{\partial N_{xy}^i}{\partial y} - I_0^i \frac{\partial^2 u_0^i}{\partial t^2} - I_1^i \frac{\partial^2 \phi_x^i}{\partial t^2} + F_x^i - F_x^{i-1} \\ &= -\delta_{iI}\left[\sum_{m\in Z} F_{xx}\delta(x-ml_x) + \sum_{n\in Z} F_{yx}\delta(y-nl_y)\right], \end{aligned} \tag{2}$$

$$\begin{aligned} &\frac{\partial N_{yy}^i}{\partial y} + \frac{\partial N_{xy}^i}{\partial x} - I_0^i \frac{\partial^2 v_0^i}{\partial t^2} - I_1^i \frac{\partial^2 \phi_y^i}{\partial t^2} + F_y^i - F_y^{i-1} \\ &= -\delta_{iI}\left[\sum_{m\in Z} F_{xy}\delta(x-ml_x) + \sum_{n\in Z} F_{yy}\delta(y-nl_y)\right] \end{aligned} \tag{3}$$

$$\begin{aligned} &\frac{\partial Q_y^i}{\partial y} + \frac{\partial Q_x^i}{\partial x} - I_0^i \frac{\partial^2 w_0^i}{\partial t^2} + F_z^i - F_z^{i-1} - P_{inc}^1 - P_s^1 + -P_t^N \\ &= -\delta_{iI}\left[\sum_{m\in Z} F_{xz}\delta(x-ml_x) + \sum_{n\in Z} F_{yz}\delta(y-nl_y)\right] \end{aligned} \tag{4}$$

$$\begin{aligned} &\frac{\partial M_{xx}^i}{\partial x} + \frac{\partial M_{xy}^i}{\partial y} - Q_x^i - I_1^i \frac{\partial^2 u_0^i}{\partial t^2} - I_2^i \frac{\partial^2 \phi_x^i}{\partial t^2} + \frac{h^i}{2}F_x^i + \frac{h^i}{2}F_x^{i-1} \\ &= -\delta_{iI}\left[\sum_{m\in Z} M_x\delta(x-ml_x)\right] \end{aligned} \tag{5}$$

$$\begin{aligned} &\frac{\partial M_{xy}^i}{\partial x} + \frac{\partial M_{yy}^i}{\partial y} - Q_y^i - I_1^i \frac{\partial^2 v_0^i}{\partial t^2} - I_2^i \frac{\partial^2 \phi_y^i}{\partial t^2} + \frac{h^i}{2}F_y^i + \frac{h^i}{2}F_y^{i-1} \\ &= -\delta_{iI}\left[\sum_{n\in Z} M_y\delta(y-nl_y)\right] \end{aligned} \tag{6}$$

where $\left(N_{xx}^i, N_{yy}^i, N_{xy}^i\right)$, $\left(Q_x^i, Q_y^i\right)$ and $\left(M_{xx}^i, M_{yy}^i, M_{xy}^i\right)$ are the force and moment resultants, respectively. P_{inc}^1, P_s^1 denote incident sound and reflected sound pressure on the first layer, and P_t^N corresponds to transmitted sound pressure on Nth layer; ($F_{x\varepsilon}$, $F_{y\varepsilon}$) $\{\varepsilon = x, y, z\}$ and (M_x, M_y) are the coupling forces and reactive torsional moments between the stiffeners and the base plate. (F_x^i, F_y^i, F_z^i) are interlayer forces of the base plate, h^i is the thickness of material layer, δ_{iI} is the Kronecker delta symbol. N is the number of total layers, then total number of interlayer forces is 3(N-1). Therefore, total 5N+3(N-1) variables can be grouped into two vectors including the displacement vector $\{\mathbf{U}\}$ and the interlayer force vector $\{\mathbf{F}\}$:

$$\begin{aligned} \{\mathbf{U}\} &= \left\{u_0^1, v_0^1, w_0^1, \phi_x^1, \phi_y^1, \ldots u_0^N, v_0^N, w_0^N, \phi_x^N, \phi_y^N\right\}^{\mathrm{T}}, \\ \{\mathbf{F}\} &= \left\{F_x^1, F_y^1, F_z^1, F_x^2, F_y^2, F_z^2, \ldots F_x^{N-1}, F_y^{N-1}, F_z^{N-1}\right\}^{\mathrm{T}}. \end{aligned} \tag{7}$$

Further, I_0^i, I_1^i and I_2 are the mass moments of inertia, defined by $(I_0^i, I_1^i, I_2^i) = \int_{z_b^i}^{z_t^i} \left(1, z, z^2\right)\rho^i dz$; where ρ^i and $z_b^i(z_t^i)$ denotes the mass density and the bottom (top) coordinate of the i th layer of the laminated composite plate, respectively. Interlayer displacement continuity condition requires:

$$u_0^i + z_i\phi_x^i = u_0^{i+1} + z_i\phi_x^{i+1}, v_0^i + z_i\phi_y^i = v_0^{i+1} + z_i\phi_y^{i+1}, w_0^i = w_0^{i+1}. \tag{8}$$

In all, the 5N+3(N-1) variables [Eq. (7)] correspond to 5N dynamic equilibrium equations [Eqs. (2)-(6)] and 3(N-1) displacement continuity equations [Eq. (8)]. Applying the Fourier transform:

$$\tilde{w}(\alpha,\beta)=\int_{-\infty}^{+\infty}\int_{-\infty}^{+\infty}w(x,y)e^{i(\alpha x+\beta y)}dxdy$$
$$w(x,y)=\frac{1}{4\pi^2}\int_{-\infty}^{+\infty}\int_{-\infty}^{+\infty}\tilde{w}(\alpha,\beta)e^{-i(\alpha x+\beta y)}d\alpha d\beta \tag{9}$$

where α and β are the transformed wavenumbers in the *x*- and *y*-direction. After Fourier transform, the governing equation can be reduced to:

$$([A_2]+i[A_1]-[A_0])\{\tilde{\mathbf{e}}\}=\{\tilde{P}_f\}+\{\tilde{P}_{Fx}\}+\{\tilde{P}_{Fy}\} \tag{10}$$

where $i=\sqrt{-1}$, the coefficient matrixes ($[A_0],[A_1],[A_2]$) are defined by Ghinet et al. [18]. Then, the hybrid variables vector, excitation forces vector, reaction forces between the base plate and the stiffeners can be written as:

$$\{\tilde{\mathrm{P}}_f\}=\left\{0,0,\tilde{P}_{inc}^1+\tilde{P}_s^1,\underbrace{0\ldots0}_{5N-4},\tilde{P}_t^N,\underbrace{0\ldots0}_{3N-3}\right\}^{\mathrm{T}},$$
$$\{\tilde{\mathrm{P}}_{Fx}\}=\left\{\tilde{F}_{xx},\tilde{F}_{xy},\tilde{F}_{xz},\tilde{M}_x,\underbrace{0\ldots0}_{8N-7}\right\}^{\mathrm{T}},\{\tilde{\mathbf{e}}\}=\{\tilde{\mathbf{U}}\ \tilde{\mathbf{F}}\}^{\mathrm{T}}, \tag{11}$$
$$\{\tilde{\mathrm{P}}_{Fy}\}=\left\{\tilde{F}_{yx},\tilde{F}_{yy},\tilde{F}_{yz},0,\tilde{M}_y,\underbrace{0\ldots0}_{8N-8}\right\}^{\mathrm{T}}.$$

2.1 The fluid loading

In Cartesian coordinates, the incident sound wave can be described as follows:

$$P_{inc}=\varepsilon_{inc}\exp\left[-ik_0(\sin\theta\sin\phi x+\sin\theta\cos\phi y+\cos\theta z)\right] \tag{12}$$

where $k_0=\omega/c_0$, c_0 is the speed of sound in the fluid. θ and ϕ are incident angle. The scattered sound pressure P_s^1 can be decomposed into two scattered pressure P_∞^1 and P_{se}^1 generated by rigid boundary and elastic motion of structure respectively.

Consider the Helmholtz equation of the acoustic fluid around:

$$\left(\frac{\partial^2}{\partial x^2}+\frac{\partial^2}{\partial y^2}+\frac{\partial^2}{\partial z^2}\right)P(x,y,z)+k_0^2P(x,y,z)=0. \tag{13}$$

Here P can be P_{se}^1 or P_t^N. Then, the coupling between plate and fluid can be expressed according to the Euler equation, $\partial P/\partial z|_{z=0}=\rho_0\omega^2w(x,y)$. Incorporating Helmholtz equation, Euler equation and Fourier transform, we obtain:

$$\begin{cases}\tilde{P}_{inc}^1(\alpha,\beta,0)=4\pi^2\delta(\alpha-k_0\sin\theta\sin\phi)\delta(\beta-k_0\sin\theta\cos\phi)\\ \tilde{P}_{se}^1(\alpha,\beta,0)=\omega^2\rho_0\tilde{w}_0^1(\alpha,\beta)/\gamma(\alpha,\beta)\\ \tilde{P}_t^N(\alpha,\beta,0)=\omega^2\rho_0\tilde{w}_0^N(\alpha,\beta)/\gamma(\alpha,\beta)\end{cases}$$
where $\gamma^2=\alpha^2+\beta^2-\omega^2/c_0^2$. (14)

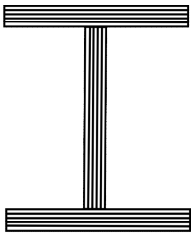

Fig. 2. Thin walled I section composite beam.

2.2 Reactive forces by stiffeners

A general governing equation of I section composite beam (as shown in Fig. 2) is introduced, which accounts for the extensional, flexural, torsional and their coupling effects. Moreover, arbitrary laminate stacking sequences (e.g. symmetric or unsymmetrical) can be handled by this theory.

Taking the stiffeners in the y-direction as an example, the coupling reactive forces between the stiffeners and the base plate can be expressed as:

$$\begin{aligned}F_{xx}&=m_0\ddot{u}+m_c\ddot{\phi}_x-E_{12}v'''+E_{22}u^{iv}+E_{24}\phi_x^{iv}-2E_{25}\phi_x''',\\ F_{xy}&=m_0\ddot{v}-E_{11}v''+E_{12}u'''-E_{13}w'''-2E_{15}\phi_x'',\\ F_{xz}&=m_0\ddot{w}+m_s\ddot{\phi}_x+E_{13}v'''+E_{33}w^{iv}+2E_{35}\phi_x''',\\ M_x&=m_c\ddot{u}-m_s\ddot{w}+\left(m_p+m_2-2m_w\right)\ddot{\phi}_x\\ &\quad-2E_{15}v'''-2E_{35}w'''+E_{24}u^{iv}+E_{44}u^{iv}-4E_{55}\phi_x'.\end{aligned} \tag{15}$$

Detailed constants can be found in Lee and Kim's paper [19]. To solve the Dirac function appeared in Eqs. (2)-(6), Poisson formula is employed [20]:

$$\sum_{m\in Z}\delta(x-ml_x)=\frac{1}{l_x}\sum_{n\in Z}\exp\left(\frac{2in\pi x}{l_x}\right). \tag{16}$$

After Fourier transform and incorporating the Eqs. (15) and (16), the reactive forces of stiffeners can be written as:

$$\{\tilde{\mathrm{F}}_x\}=\begin{Bmatrix}\tilde{F}_{xx}\\ \tilde{F}_{xy}\\ \tilde{F}_{xz}\\ \tilde{M}_x\end{Bmatrix}=\begin{bmatrix}\tilde{z}_x^{11}&\tilde{z}_x^{12}&\tilde{z}_x^{13}&\tilde{z}_x^{14}&0\\ \tilde{z}_x^{21}&\tilde{z}_x^{22}&\tilde{z}_x^{23}&\tilde{z}_x^{24}&0\\ \tilde{z}_x^{31}&\tilde{z}_x^{32}&\tilde{z}_x^{33}&\tilde{z}_x^{34}&0\\ \tilde{z}_x^{41}&\tilde{z}_x^{42}&\tilde{z}_x^{43}&\tilde{z}_x^{44}&0\end{bmatrix}\begin{Bmatrix}\sum_{m\in Z}\tilde{u}_0^1(\alpha_m,\beta)\\ \sum_{m\in Z}\tilde{v}_0^1(\alpha_m,\beta)\\ \sum_{m\in Z}\tilde{w}_0^1(\alpha_m,\beta)\\ \sum_{m\in Z}\tilde{\phi}_x^1(\alpha_m,\beta)\\ \sum_{m\in Z}\tilde{\phi}_y^1(\alpha_m,\beta)\end{Bmatrix}$$
$$=A(\alpha,\beta)\sum_{m\in Z}W(\alpha_m,\beta) \tag{17}$$

where the coefficient $\tilde{z}_x^{ij}(i,j=1\sim4)$ represents the transformed coefficient matrix elements. $A(\alpha,\beta)$, $\sum_{m\in Z}W(\alpha_m,\beta)$ ($\alpha_m=\alpha+2m\pi/l_x$) denotes coefficient matrix and displacement vector, respectively. With $\beta_n=\beta+2n\pi/l_y$, the reactive forces of stiffeners in x-direction are given by:

$$\left\{\tilde{\mathrm{F}}_y\right\}=\begin{Bmatrix}\tilde{F}_{yx}\\ \tilde{F}_{yy}\\ \tilde{F}_{yz}\\ \tilde{M}_y\end{Bmatrix}=\begin{bmatrix}\tilde{z}_y^{11} & \tilde{z}_y^{12} & \tilde{z}_y^{13} & 0 & \tilde{z}_y^{14}\\ \tilde{z}_y^{21} & \tilde{z}_y^{22} & \tilde{z}_y^{23} & 0 & \tilde{z}_y^{24}\\ \tilde{z}_y^{31} & \tilde{z}_y^{32} & \tilde{z}_y^{33} & 0 & \tilde{z}_y^{34}\\ \tilde{z}_y^{41} & \tilde{z}_y^{42} & \tilde{z}_y^{43} & 0 & \tilde{z}_y^{34}\end{bmatrix}\begin{Bmatrix}\sum_{n\in Z}\tilde{u}_0^1(\alpha,\beta_n)\\ \sum_{n\in Z}\tilde{v}_0^1(\alpha,\beta_n)\\ \sum_{n\in Z}\tilde{w}_0^1(\alpha,\beta_n)\\ \sum_{n\in Z}\tilde{\phi}_x^1(\alpha,\beta_n)\\ \sum_{n\in Z}\tilde{\phi}_y^1(\alpha,\beta_n)\end{Bmatrix}$$
$$=B(\alpha,\beta)\sum_{n\in Z}W(\alpha,\beta_n). \tag{18}$$

2.3 Solution in wavenumber domain

Combining Eqs. (17), (18) and (10), and introducing the abbreviated equations defined in Eqs. (17) and (18), the resultant governing equation in wavenumber domain is:

$$W(\alpha,\beta)=f(\alpha,\beta)-A(\alpha,\beta)\sum_{m\in Z}W(\alpha_m,\beta)-B(\alpha,\beta)\sum_{n\in Z}W(\alpha,\beta_n) \tag{19}$$

which contains only one set of unknowns $W(\alpha_m,\beta_n)$ with $m=-\infty$ to $+\infty$ and $n=-\infty$ to $+\infty$. Insofar as the solution converges, the equation can be solved by truncation. In other words, (m,n) only take the values in a finite range of $m=-\hat{m}$ to $\hat{m}$ and $n=-\hat{n}$ to $\hat{n}$, then the resulting equations are simplified to simultaneous equations containing a finite number (i.e. $2MN$, where $M=2\hat{m}+1$, $N=2\hat{n}+1$). Remarkably, intrinsic physical mechanism of this computational method [1] is that the flexural wave with wavenumber (α,β) is able to excite the waves with wavenumber components ($\alpha+2m\pi/l_x$, $\beta+2n\pi/l_y$). By the way, the inherent convergence rule say that once solution was convergent at a given frequency, then it will be convergent for all frequencies lower than that Ref. [8]. Therefore, enough terms ($M=N=21$) have been chosen to ensure the convergence of the results at the highest frequency 5000 Hz of interest within the error bound of 0.5 dB.

2.4 Sound transmission loss

Considering an infinite structure, the incident sound intensity can be defined as follows:

$$W_{inc}=\frac{1}{2}|P_{inc}|^2\frac{\cos\theta}{\rho_0c_0}. \tag{20}$$

As for the transmitted sound intensity, it can be given by using the displacements in wavenumber domain [21]:

$$W_{trans}=\frac{\rho_0\omega^3}{8\pi^2}\sum_{\left(\alpha_m^2+\beta_n^2\right)<k_0^2}\frac{|w(\alpha_m,\beta_n)|^2}{\sqrt{k_0^2-\alpha_m^2-\beta_n^2}}. \tag{21}$$

Hence, the sound transmissivity at frequency ω and incidence angle (θ,ϕ) is then:

$$\tau(\omega,\theta,\phi)=\frac{W_{trans}}{W_{inc}}. \tag{22}$$

When diffused sound field is taken into account, the sound transmissivity can be given by:

$$\tau_{diff}(\omega)=\frac{\int_0^{2\pi}\int_0^{\theta_{\max}}\tau(\omega,\theta,\phi)\sin\theta\cos\theta d\theta d\phi}{\int_0^{2\pi}\int_0^{\theta_{\max}}\sin\theta\cos\theta d\theta d\phi}. \tag{23}$$

Thereby, sound transmission loss is expressed as

$$\mathrm{STL}=-10\log_{10}\left[\tau_{diff}(\omega)\right]. \tag{24}$$

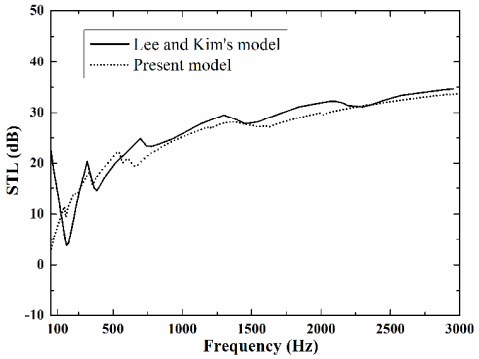

Fig. 3. Comparison between the theoretical predictions and Lee and Kim's theoretical results [22].

3. Validation of theoretical modeling

To the authors' knowledge, no direct experimental data regarding the STL of orthogonally stiffened composite panel exist in the open literature. To validate the present theoretical model, the model predictions are firstly compared with published theoretical results [22] for unidirectional stiffened thin homogeneous panel as shown in Fig. 3.

It can be seen that the two curves coincide well in a wide

frequency range at first glance, which thus validates the present model to a large extent. The existing deviation between these two curves is mainly attributed to different modeling assumptions. Specifically, in Lee and Kim's work [22], the stiffeners are represented by a series of lumped mass and springs linked to ground. In contrast, beam theory is employed to model the vibration of the stiffener in the present paper. Moreover, in the low frequency range (approximately lower than 120 Hz), the equivalent springs directly linked to ground by Lee and Kim [22] improves the whole rigidity of structure and thus overestimates the STL significantly. In the frequency range higher than 120 Hz, the existing discrepancy between these two models is attributed to the different stiffener approximation. In fact, the fluctuations on the current STL curves come from the flexural wave reflection and transmission by the stiffeners, while the resulting curves of unstiffened plates are smooth. Generally, the present model gives reasonable predictions under the hypothesis of beam stiffeners.

4. Parameter investigation and discussions

After validation of the theoretical model, parameter investigations are performed in the following sections to explore the sound transmission properties of the structure, which should be beneficial for the design of the orthogonally stiffened laminated composite plate in practice. Material and geometry properties of the considered structure are listed in Table 1, where the same fiber/epoxy has been chosen for the base plate and the stiffeners. Unless otherwise stated, incident angles hold at $\theta = \phi = 45^{\circ}$, the stacking geometry of the composite stiffeners (five layers) are assumed to be [0°/0°/0°/0°/0°].

4.1 Different plate theories

As stated above, the present layerwise shear deformable theory can be degraded to the first order shear deformable theory (FSDT) if the number of total layers is assumed to be one. Then, two typical layer configurations (one layer [45°] and three layers [45°/45°/45°]) are chosen to illustrate the difference between the two different plate theories, as shown in Fig. 4.

As for an infinite unstiffened plate, it is known that its STL curve can be divided into three regions from low to high frequency, including mass-controlled region, damping-controlled region and stiffness-controlled region [23]. While for stiffened composite plate, these are three similar regions illustrated in Fig. 4, which include the mass-controlled region and damping-controlled region by the base plate, as well as the stiffness-controlled region by the base plate and stiffeners. In other words, the influence of stiffeners is mainly limited to the frequency range higher than the coincidence frequency. Besides, the coincidence frequency for an isotropic plate can be calculated following the formula $f_c = \left(c_0^2 / 2\pi h \sin^2\theta\right)\sqrt{12\rho(1-\upsilon^2)/E}$ in the Ref. [24], which helps to understand the influence of parameters on coincidence frequency here. In order to achieve an accurate result for the coincidence frequency of composite plate, a more sophisticated model based on the first order shear deformable theory [25] may be applied.

Table 1. Material and geometry properties.

Base plate (fiberglass/epoxy)						Acoustic fluid	
E_1	E_2	G_{12}	η	h	ρ	ρ_0	C_0
56 GPa	13 GPa	4.2 GPa	0.02	0.01 m	1900 kg/m^3	1.21 kg/m^3	343 m/s
I-section composite stiffeners							
Thickness h_0		Flange width		Web width		Spacing $l_x = l_y$	
0.001 m		0.01 m		0.02 m		0.25 m	

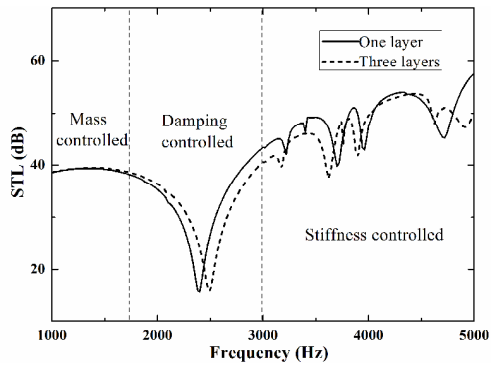

Fig. 4. Sound transmission loss of composite plate with one layer and three layers.

Moreover, it can be observed from Fig. 4 that the one layer and three layers configurations coincide well owing to the same mass density of the two structures in the mass-controlled region. While, there exist significant differences between the two curves in damping-controlled and stiffness-controlled regions, which actually demonstrates that the layewise shear deformable theory employed here can give more accurate results. Of course, the present model with more layers is capable of obtaining more accurate results while requiring larger computational efforts. As a compromise between the accuracy and the computational cost, the three layer configuration is used in the subsequent analysis.

4.2 Different beam stiffener theories

For all metallic stiffened plate, only reactive forces from the stiffener flexural motion is usually considered, which lies on the fact that the influence of other motion forms can be neglected [5]. However, for all composite stiffened structure, this approximation does not work since coupling effect exists due to the material anisotropy. In the present work, the extensional, flexural and torsional motions of the composite stiffeners are taken into account in Eq. (11). To explore the influences of the coupling effects of the composite stiffeners, the sound transmission losses of the whole structure with complete motions and with only flexural motion of the composite stiffeners are compared in Fig. 5. As shown in Fig. 5, it is found that there appears discrepancy between the two cases in stiffness-

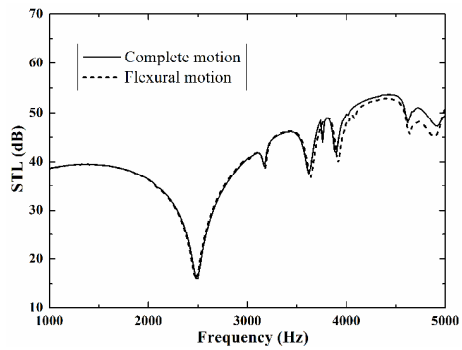

Fig. 5. Comparison between the results considering the complete motion and the only flexural motion of the composite stiffeners.

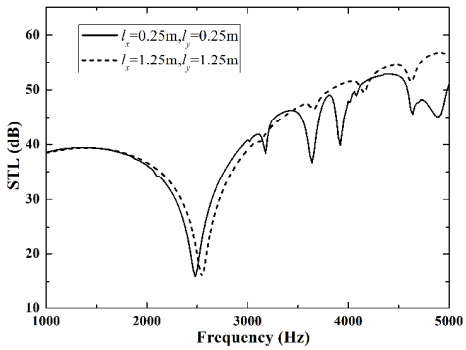

Fig. 6. Influence of stiffener spacing on sound transmission loss of the whole structure.

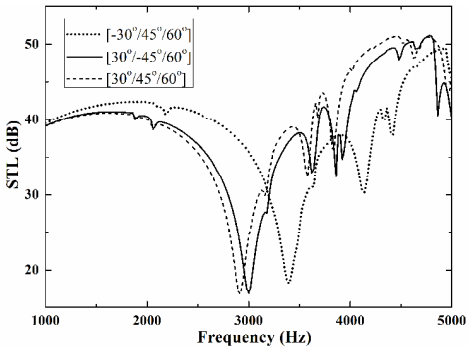

Fig. 7. Influence of stacking geometry of base plate on sound transmission loss.

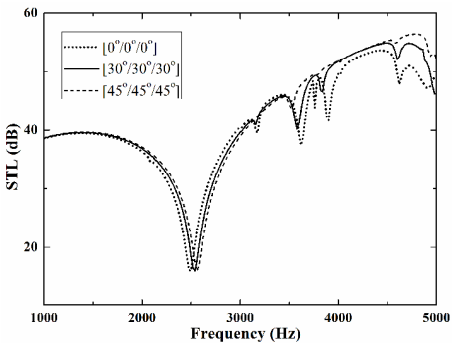

Fig. 8. Influence of stacking geometry of stiffeners on sound transmission loss.

controlled region, which actually proves the necessity of accurately considering the complete motions of the composite stiffeners.

4.3 Influence of stiffener spacing

Periodic stiffener spacing is a key geometry parameter to determine the configuration of the orthogonally stiffened plates. As depicted in Fig. 6, two different spacings have been chosen to examine the influence of the stiffeners spacings on structural sound transmission loss. In the damping controlled region, plate bending wave length greatly exceeds stiffener spacing, where structure works similar to unstiffened plate with equivalent static stiffness as stated by Fahy [23]. Therefore, as shown in Fig. 6, the coincidence frequency shifts to higher frequency with the increase of the stiffener spacing because of the decreased equivalent bending stiffness. As for the peaks and dips appearing in STL curves in stiffness-controlled region, it is shown that larger stiffener spacing produces smother sound transmission curve, which results from the fact the structure with larger stiffener spacing owns sparser modal density compared to its companions.

4.4 Different stacking geometry

Once the materials of laminated composite plates are chosen, stacking geometry will be the most important variable parameter which can change the overall stiffness of the structure. This kind of designability of composite material is one of the core reasons explaining the widespread applications of composites. Sound transmission losses for orthogonally stiffened llaminated composite plates with three typical kind of stacking geometries of the base plate are plotted in Fig. 7. In very low frequency, the three curves coincide well in mass-controlled region. With the increase of the frequency, the three curves display significant discrepancies especially for the laminate scheme [-30°/45°/60°], which shifts the coincidence frequency to higher frequency remarkably. This is because the bending stiffness is highly determined by the stacking geometry, which thus provides a feasible approach to amend the acoustic performances of laminated composites in the way of changing the stacking geometry of the base plate in a wide frequency range.

Moreover, the sound transmission losses of the stiffened laminated composite plates with three typical kinds of stacking geometries of the composite stiffeners are plotted in Fig. 8. Compared to the influence of the stacking geometry of the base plate, the stacking geometry of the stiffeners has a smaller influence on the structure sound transmission. In other words, the influence of the stacking geometry of the stiffeners is mainly limited to the stiffness-controlled region. It actually tells that it may not effectively work for amending the vibroacoustic behavior of the stiffened composite plates by adjusting the stacking geometry of the composite stiffeners.

5. Conclusions

A theoretical model for sound transmission across orthogonally stiffened composite plate has been developed by using the Fourier transform and a layerwise shear deformable theory. After validation of the model by comparing with existing theoretical results, the influences of several key parameters of the system on STL are quantified including stiffeners spacing and stacking geometry. The results show that present layerwise shear deformable theory will give more accurate results especially at high frequency. Stacking geometry has little influence on sound transmission loss in low frequency, but which plays a significant role in transmission loss in higher frequency and becomes an important design parameter to tailor the structural sound insulation property. In general, the present model provides an efficient theoretical approach to predict the transmission loss of stiffened composite plate.

Acknowledgment

This work is supported by the National Basic Research Program of China (2011CB610300), the National Natural Science Foundation of China (11102148 and 11321062), and the Fundamental Research Funds for Central Universities of China (xjj2011005).

References

[1] F. X. Xin and T. J. Lu, Analytical modeling of wave propagation in orthogonally rib-stiffened sandwich structures: Sound radiation, *Computers & Structures*, 89 (5-6) (2010) 507-16.

[2] D. J. Mead and K. K. Pujara, Space-harmonic analysis of periodically supported beams: response to convected random loading, *Journal of Sound and Vibration*, 14 (4) (1971) 525-32.

[3] B. R. Mace, Sound radiation from fluid loaded orthogonally stiffened plates, *Journal of Sound and Vibration*, 79 (3) (1981) 439-52.

[4] B. R. Mace, Periodically stiffened fluid-loaded plates, I: Response to convected harmonic pressure and free wave propagation, *Journal of Sound and Vibration,* 73 (4) (1980) 473-86.

[5] B. R. Mace, Sound radiation from a plate reinforced by two sets of parallel stiffeners, *Journal of Sound and Vibration*, 71 (3) (1980) 435-41.

[6] T. R. Lin and J. Pan, A closed form solution for the dynamic response of finite ribbed plates, *Journal of the Acoustical Society of America*, 119 (2) (2006)917-25.

[7] C. Guigou-Carter and M. Villot, Modelling of sound transmission through lightweight elements with stiffeners, *Building Acoustics*, 10 (3) (2003)193-209.

[8] F. X. Xin and T. J. Lu, Transmission loss of orthogonally rib-stiffened double-panel structures with cavity absorption, *Journal of the Acoustical Society of America*, 129 (4) (2011) 1919-1934.

[9] F. X. Xin and T. J. Lu, Sound radiation of orthogonally rib-stiffened sandwich structures with cavity absorption, *Composites Science and Technology*, 70 (15) (2010) 2198-206.

[10] D. J. Mead, Wave propagation in continuous periodic structures: Research contributions from Southampton, 1964-1995, *Journal of Sound and Vibration*, 190 (3) (1996) 495-524.

[11] J. Brunskog and P. Hammer, Prediction models of impact sound insulation on timber floor structures; A literature survey, *Building Acoustics*, 7 (2) (200) 89-112.

[12] A. Pellicier and N. Trompette, A review of analytical methods, based on the wave approach to compute partitions transmission loss, *Applied Acoustics*, 68 (10) (2007) 1192-212.

[13] J. Wang, T. J. Lu, J. Woodhouse, R. S. Langley and J. Evans, Sound transmission through lightweight double-leaf partitions: Theoretical modeling, *Journal of Sound and Vibration*, 286 (4-5) (2005) 817-47.

[14] S. M. Huybrechts, T. E. Meink, P. M. Wegner and J. M. Ganley, Manufacturing theory for advanced grid stiffened structures, *Composites Part A: Applied Science and Manufacturing*, 33 (2) (2002) 155-61.

[15] X. W. Yin, L. J. Liu, H. X. Hua and R. Y. Shen, Acoustic radiation from an infinite laminated composite cylindrical shell with doubly periodic rings, *Journal of Vibration and Acoustics-Transactions of the ASME*, 131 (1) (2009) 011005.

[16] X. Yin, X. Gu, H. Cui and R. Shen, Acoustic radiation from a laminated composite plate reinforced by doubly periodic parallel stiffeners, *Journal of Sound and Vibration*, 306 (3-5) (2007) 877-89.

[17] A. Mejdi, J. Legault and N. Atalla, Transmission loss of periodically stiffened laminate composite panels: Shear deformation and in-plane interaction effects, *Journal of the Acoustical Society of America*, 131 (1) (2012) 174-185.

[18] S. Ghinet and N. Atalla, Modeling thick composite laminate and sandwich structures with linear viscoelastic damping, *Computers & Structures*, 89 (15) (2011) 1547-61.

[19] J. Lee and S. E. Kim, Flexural–torsional buckling of thin-walled I-section composites, *Computers & Structures*, 79 (10) (2001) 987-95.

[20] D. Takahashi, Sound radiation from periodically connected double-plate structures, *Journal of Sound and Vibration*, 90 (4) (1983) 541-57.

[21] L. Cremer L, M. Heckl and B. A. T. Petersson, *Structure-borne sound*, 3ed: Springer, Berlin, Germany (2005).

[22] J. H. Lee and J. Kim, Analysis of sound transmission through periodically stiffened panels by space-harmonic expansion method, *Journal of Sound and Vibration*, 251 (2) (2002) 349-66.

[23] F. Fahy and P. Gardonio, *Sound and structural vibration: radiation, transmission and response*, 2 ed: Academic Press, Oxford, UK (2007).

[24] F. X. Xin and T. J. Lu, Analytical modeling of fluid loaded orthogonally rib-stiffened sandwich structures: Sound transmission, *Journal of the Mechanics and Physics of Solids*, 58 (9) (2010)1374-96.

[25] S. Ghinet and N. Atalla, H. Osman, Diffuse field transmission into infinite sandwich composite and laminate composite cylinders, *Journal of Sound and Vibration*, 289 (4-5) (2005) 745-78.

Fengxian Xin received his Ph.D. from Xi'an Jiaotong University in 2011. He is currently an Associate Professor of State Key Laboratory for Mechanical Structure Strength and Vibration in Xi'an Jiaotong University. His research interests include vibration, acoustic and thermal property of lightweight structures.

Cheng Shen received his Ph.D. from Xi'an Jiaotong University in 2014. Recently, he joined College of Energy and Power Engineering, Nanjing University of Aeronautics and Astronautics as a lecturer. His major interest is vibration and acoustic property of metallic and composite lightweight structures.